Citrate-based fluorometric sensor for multi-halide sensing

Dingbowen Wang [a,1], Tunan Xia [b,1], Yuqi Wang [a], Yizhu Chen [b], Chenji Zhang [b], William Murray [b], Adam Thomas Schultz [a], Zhiwen Liu [b,**], Jian Yang [a,*]

[a] *Department of Biomedical Engineering, Materials Research Institute, The Huck Institutes of the Life Sciences, The Pennsylvania State University, University Park, PA, 16802, USA*
[b] *Department of Electrical Engineering, Materials Research Institute, The Pennsylvania State University, University Park, PA, 16802, USA*

ARTICLE INFO

ABSTRACT

Halides play important roles in human health and environmental monitoring. However, different halides interfere with each other in current measurement methods. Simultaneous sensing of multiple halides in a fast and low-cost manner remains a challenge. Here, we report a fluorometric multi-halide sensing method by using a single citrate-based fluorophore, CA-Cys, on a custom-made portable device. The fluorescence emitted by CA-Cys is quenched due to the dynamic quenching of halide ions; the sensitivities vary from halide types and pH, providing the capability to obtain multiple Stern-Volmer equations at various pH values. The concentration of each halide can then be obtained by solving the resultant set of equations. A mM scale detection limit is demonstrated, which is suitable for halide wastewater monitoring. A proof-of-concept smartphone-based portable device is also fabricated and tested. The results from the fluorometer and portable device indicated that our multi-halide system is promising for real-world multi-halide sensing applications. This work represents a new direction in developing portable, low-cost, and simultaneous multi-halide sensing technologies.

1. Introduction

Halides are anion forms of halogen atoms located in Group VII of the periodic table. The halides, including fluoride (F⁻), chloride (Cl⁻), bromide (Br⁻), iodide (I⁻) and astatide (At⁻), play an essential role in various fields, such as health care, environmental monitoring, and industrial applications, except the highly radiative and rare astatine. Cl⁻ is a major component of natural waters, which sources from the ocean, dissolution of evaporite rocks naturally, or from urban, industrial, and agricultural wastewaters anthropogenically [1]. Br⁻ is a common but minor constitute of natural waters, which sources from the ocean and dissolution of evaporite rocks naturally similar to Cl⁻, and from potassium ore mining, production of fire retardant agents, and the use of fertilizers and pesticides in agriculture anthropogenically [1–3]. Cl⁻ and I⁻ are essential electrolytes that maintain homeostasis within the human body, where abnormal levels may indicate various diseases. For example, abnormal Cl⁻ concentrations in biological fluids, such as sweat, urine, serum, and cerebral spinal fluid (CSF) are indicators of cystic fibrosis (CF), metabolic alkalosis, Addison's disease, and amyotrophic lateral sclerosis (ALS), respectively [4–6]. I⁻ is essential to maintain normal functions of the thyroid since two thyroid

hormones, triiodothyronine (T₃) and thyroxine (T₄), are iodine-containing and synthesized by using I⁻. Abnormal iodide levels, either too high or too low, can cause thyroid dysfunction, resulting in diseases, such as hyperthyroidism and hypothyroidism [7]. It is widely accepted that bromine is not an essential element and Br⁻ is not necessary to maintain human health (except one publication so far [8]). Studies have shown that Br⁻ has a low degree of toxicity and is not a toxicological concern in nutrition [9]. However, Br⁻ can react with chlorine and ozone in drinking water, forming brominated and mixed chloro-bromo byproducts, such as trihalomethanes and halogenated acetic acids and bromate, respectively [9–11]. Most of the aforementioned brominated byproducts have been shown to have carcinogenic or teratogenic effects and are even worse than their chlorinated counterparts [12–18].

Multi-halide sensing is critical for many applications. The Cl⁻/Br⁻ ratio helps identify the history of freshwater or groundwater systems and distinguishes different origins of contaminants since the Cl⁻/Br⁻ ratio should be a constant in a natural water system until a new source of water with a different ratio is added [1,19]. Besides Cl⁻, higher levels of Br⁻ and I⁻ have also been found in various body fluids of CF patients or even CF carriers (someone with one normal CF gene and one faulty CF gene),

probably due to the abnormal voltage gradient generated by poor chloride reabsorption, which affects the reabsorption of other ions, particularly for ions with smaller hydrated radii such as bromide and iodide that are also permeable to chloride channels [20–23]. Moreover, sweat Br⁻ elevation has been reported in patients with bromism who suffer from occupational hazards involving methyl bromide in fumigants and fire extinguishers and who administrate certain laxatives, anticonvulsants, and cough suppressants (such as Dextromethorphan) [24]. In the aforementioned cases, multi-halide sensing is needed and helpful to either acquire the concentration of each halide or distinguish relatively lower concentration halide from the high Cl⁻ background. The current fully automated halide determination methods include ion-selective electrodes (ISE), coulometry, and colorimetry. However, all three methods suffer from poor halide selectivity [25–27]. In ISE, for example, bromide and iodide produce signals 10^2 and 10^3 times greater than chloride, respectively [28,29]. Chloridometers based on ISE typically cost several thousand dollars, while automated analyzers based on coulometry or colorimetry can cost tens of thousands. On the other hand, sophisticated analytical methods, such as anion exchange chromatography, do enable high halide selectivity, but at the cost of high maintenance, expensive equipment, and manual labor of trained technicians [25,30–32]. Therefore, efforts have been devoted to developing new halide sensors. Although the ideal approach to halide sensing is direct chelation, there are no selective halide chelators to date [33]. Recently developed sensors include a chloride chelating conjugate that utilizes a rhodium(III) center [34], squaramide derivatives with a fluorescence "turn-on" response to chloride [35], and aggregation-based chloride sensors based on bis(aryl ethynyl)pyridine compounds [36], which all possess highly sensitive responses to chloride but suffer from significant interferences from other anions. Aqueous halide sensing is another challenge for developing new halide sensors. Halide sensors are generally pure organic compounds requiring organic solvents or stabilizers to maintain solubility or functionality [34,35], which hinders their performance in real-world applications, such as body fluids examination and water quality monitoring. In meeting the aforementioned challenges, fluorometric sensors may play a vital role in halide sensing applications as fluorescence offers high sensitivity, rapid response kinetics, low technical complexity, and a particularly high signal-to-noise ratio due to minimal background interference compared to other colorimetric or coulometric methods [37]. However, existing fluorometric halide sensors, quinolinium-based dyes and yellow fluorescent proteins, suffer from narrow linear range, low fluorescence quantum yield, poor photostability and high costs, thereby limiting their applications [38–42]. Thus, there is an urgent need for a low-cost, highly selective, highly photostable and reliable fluorometric method in aqueous conditions for multi-halide sensing.

In 2017, we reported a novel fluorometric Cl⁻ sensing method for CF diagnosis application and proposed the concept for multi-halide sensing [43]. In this work, a novel fluorometric multi-halide sensing method based on a citrate-derived fluorophore is presented, and a smartphone-based portable device is demonstrated. In addition, artificial multi-halide solutions are tested for the proof of concept of both the method and the portable device. To the best of our knowledge, this is the first report that a single fluorophore is used to selectively detect multiple halides simultaneously based on a dynamic quenching mechanism. Due to the significant impacts of halide ions in various fields, it is expected that this work paves the way for many future applications where simultaneous multi-halide sensing is desirable.

2. Experimental and methodological

2.1. Materials

Water with a resistivity of 18.2 MΩ/cm was acquired from a Thermo Scientific Barnstead E-Pure Ultrapure Water Purification system. All reagents were purchased from Sigma Aldrich and used without additional purification.

2.2. Synthesis of citrate-based fluorophores

The synthesis of citrate-based fluorophores follows our previous publications via a one-pot reaction of citric acid and a primary amine compound dissolved in water [43,44]. In the case of CA-Cys, 10 mmol each of citric acid (1.92 g) and L-cysteine (1.21 g) were added to a 50 mL round-bottom flask with 10 mL distilled water. The reaction was conducted at 140 °C for 1 h and terminated by adding 5 mL of distilled water to dissolve the products. The purification was performed through recrystallization twice by cooling saturated CA-Cys solution at 4 °C overnight. The synthesis scheme of CA-Cys is shown in Fig. 2 (a). To confirm the chemical structure and examine the purity of the as-prepared CA-Cys, ¹H NMR (DMSO-d₆) spectrum was recorded and the peaks at chemical shifts δ 6.58 (d, 1H), 5.48 (d, 1H), 3.90 (t, 1H), 3.60 (d, 2H) were assigned to the protons on CA-Cys as shown in Fig. 2 (a). The purity of CA-Cys was calculated using a relative quantification method (also termed as 100% quantitative ¹H NMR method, 100% qHNMR method) as previously described [45], which is 98.0%.

2.3. Photophysical and optical properties characterizations of CA-Cys

To investigate the photoluminescence (PL) of CA-Cys and determine the ideal wavelengths for sensing applications, the fluorescence excitation and emission spectra as well as the quantum yield of CA-Cys were measured. The optical density (OD) of the solutions was kept to 0.1 in these measurements. Additionally, to better quantify the color changes, the CIE 1931 chromaticity coordinates of neutral state and acidic state CA-Cys solutions were calculated. The optical density (absorbance) was obtained from a Tecan Infinite 200 PRO plate reader equipped with a cuvette port. The steady-state fluorescence spectra were collected on a Horiba FluoroMax-4 spectrofluorophotometer. The quantum yield measurement was also carried out on a Horiba FluoroMax-4 equipped with a Quanta-φ F-3029 integrating sphere.

2.4. Mechanism of multi-halide sensing

Dynamic quenching (also known as collisional quenching) is a type of quenching resulting from collisional encounters between a fluorophore and a quencher [37]. It was already known that pH conditions below 2.4 can open the accessibility of CA-Cys to dynamic quenching due to the excited state protonation of 5-carbonyl group [43] (the position number of CA-Cys is shown in Fig. 2 (b) and in the following, CA-Cys at a pH greater than 2.4 is called neutral state CA-Cys while CA-Cys at a pH less than 2.4 is called acidic state CA-Cys). Furthermore, different halides possess different sensitivities at the same pH, and the sensitivities increase with acidity [43]. The pH-dependent halide sensitivities inspired us to create more than one modified Stern-Volmer (SV) equation under different pH conditions with the same multi-halide sample. By solving the equation set, the concentration of each halide can be obtained (Fig. 1).

The original SV equation is shown below:

$$\frac{I_0}{I} = k_q \tau_0 [Q] + 1 = K_{sv}[Q] + 1 \tag{1}$$

where I_0 and I are the fluorescence intensities in the absence and presence of the quencher, respectively, k_q is the bimolecular quenching constant, τ_0 is the lifetime of the fluorophore in the absence of the quencher, and $[Q]$ is the concentration of the quencher. The Stern-Volmer quenching constant is given by $K_{sv} = k_q \tau_0$. In our previous work, we have derived a modified SV equation (Eqn (2)) [43], which contains a H⁺ term, listed below:

$$\frac{I_0}{I_{H,Q}} = K_{sv(Q)}[Q] + K_{sv(H^+)}[H^+] + 1 \tag{2}$$

where $I_{H,Q}$ is the fluorescence intensity in the presence of both acid and halide and $K_{sv(H^+)}$ is the Stern-Volmer quenching constant of proton. By
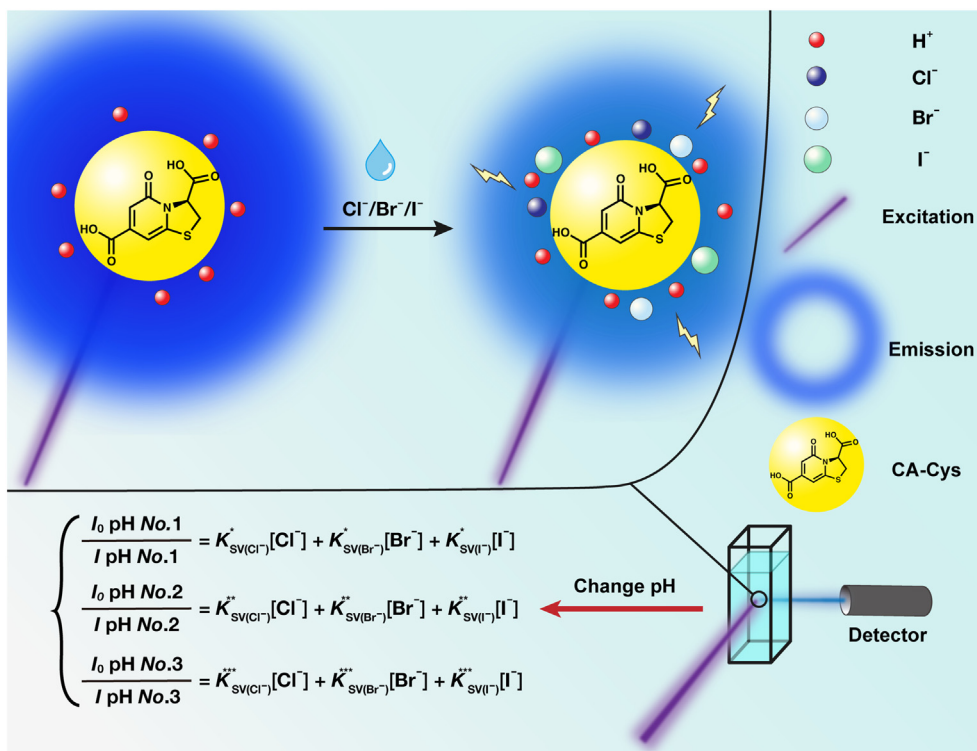
Fig. 1. Schematic illustration of the proposed multi-halide sensing mechanism and method. The H$^+$ opens the dynamic quenching of CA-Cys on halides. By varying pH, the fluorescence signals are collected and multiple equations can be obtained due to the distinct sensitivities for each halide. The concentration of each halide can be obtained by solving the resultant set of equations.
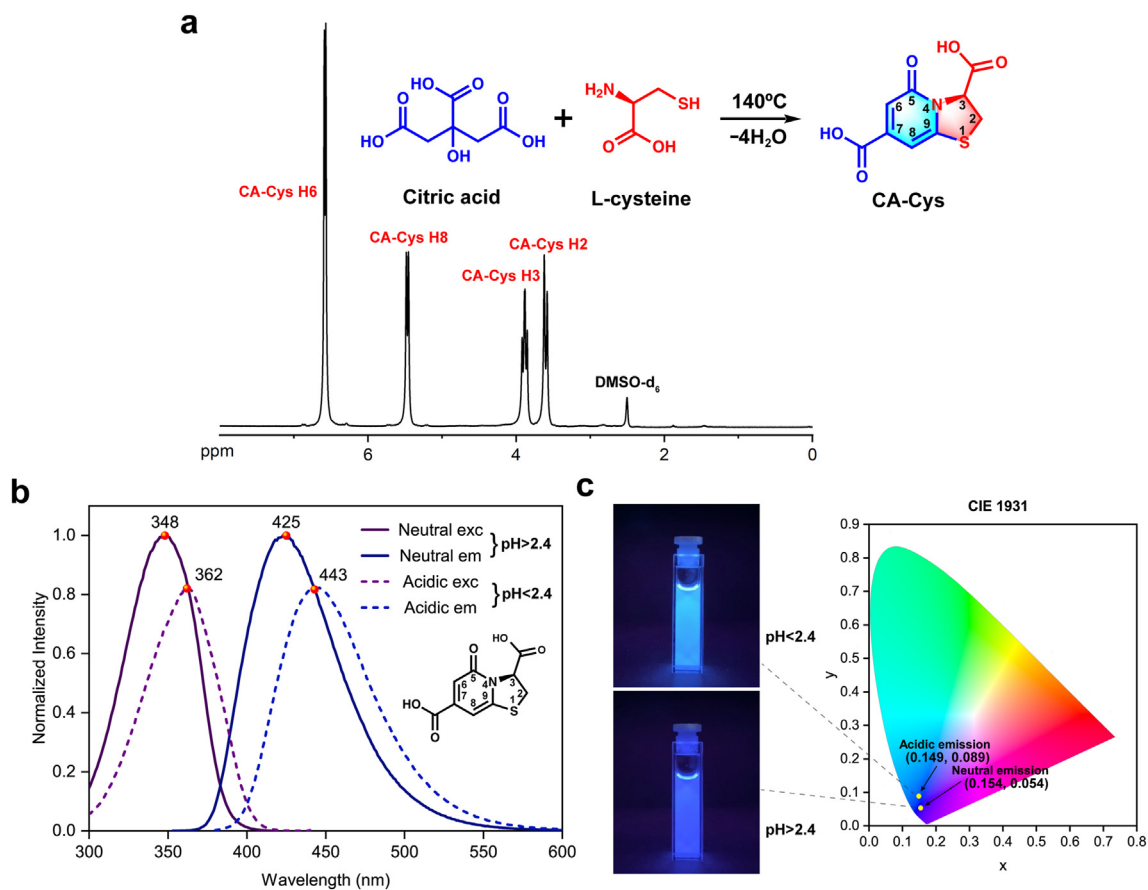

Fig. 2. The synthesis and optical properties of CA-Cys. (a) The one-pot synthesis of CA-Cys from citric acid and L-cysteine; and ^{1}H NMR spectrum of CA-Cys. (b) The fluorescence spectra of CA-Cys in its neutral (pH > 2.4) and acidic states (pH < 2.4). The pH conditions below 2.4 open the accessibility of CA-Cys to dynamic quenching due to the excited state protonation of 5-carbonyl group. (c) The fluorescence images of CA-Cys in cuvettes and their CIE 1931 chromaticity coordinates at neutral (pH > 2.4) and acidic states (pH < 2.4).

dividing $K_{sv(H^+)}[H^+]+1$ on both sides, a modified SV equation is derived:

$$\frac{I_0^*}{I^*} = K_{sv(Q)}^*[Q] + 1 \tag{3}$$

where I_0^* is the fluorescence intensity in the absence of any halide at a certain pH (with a certain concentration of H_2SO_4), I^* is the fluorescence intensity in the presence of halide(s) at the same above pH and $K_{sv(Q)}^*$ is the Stern-Volmer quenching constant of a certain halide at the same above pH. We have already proven that each halide is an independent quencher from the others in our previous work [43]. Thus, terms of different halides can be summed up without any intervention term. Then Cl^-, Br^- and I^- concentration can be solved simultaneously by establishing multiple equations under various pH conditions. The entire equation set is given below and in Fig. 1:

$$\begin{cases} \dfrac{I_0 \; pH \, No. 1}{I \; pH \, No. 1} = K_{sv(Cl^-)}^*[Cl^-] + K_{sv(Br^-)}^*[Br^-] + K_{sv(I^-)}^*[I^-] \\[2mm] \dfrac{I_0 \; pH \, No. 2}{I \; pH \, No. 2} = K_{sv(Cl^-)}^{**}[Cl^-] + K_{sv(Br^-)}^{**}[Br^-] + K_{sv(I^-)}^{**}[I^-] \\[2mm] \dfrac{I_0 \; pH \, No. 3}{I \; pH \, No. 3} = K_{sv(Cl^-)}^{***}[Cl^-] + K_{sv(Br^-)}^{***}[Br^-] + K_{sv(I^-)}^{***}[I^-] \end{cases} \tag{4}$$

It is noted that not all three halides are necessary. A halide term can be removed if this halide is absent in the solution.

2.5. Fabrication of smartphone-based portable device for multi-halide sensing

A portable device was developed, which worked as a smartphone accessory and was equipped with a UV light emitting diode (LED) to excite CA-Cys. The fluorescence was collected by the smartphone camera for the quantitative determination of halide solutions. The UV LED excitation light source (365 nm excitation, maximum 10 mW output power) was soldered onto a printed circuit board, adjoined to an aluminum block for heat dissipation, and powered by a 9 V battery. To maintain a stable operating temperature and reliable device performance, a 7-Ω high power resistor was used to control the voltage and current supplied to the LED, limiting the applied voltage to 4.1 V and current to 700 mA as specified by the manufacturer. An HTC One M9 smartphone was used, with its camera optimized with an exposure time of 100 ms, ISO of 400, and capture a digital negative (DNG) raw image of a cuvette sample placed very close to the camera. Our device design can accommodate most types of smartphones given that the camera parameters (e.g. white balance, gain level, exposure time, and focal lengths) are fixed during the measurements. The fluorescence intensity of each measurement was determined by the summation of the total pixel values of the captured fluorescence pattern. This blue fluorescence was collected by the smartphone camera in the transmission direction. In addition, a 441.6 nm band-pass filter was used (L441.6–10 Ø1" Laser Line Filter) to remove the excitation light since the fluorescence emission wavelength of CA-Cys is centered at 443 nm. The device was 3D printed (via Solidoodle) out of black acrylonitrile-butadiene-styrene plastic.

It should be noted that, for fluorescence measurements with a fluorometer, the detector recorded the emission light in a direction perpendicular to the excitation light (90° geometry), while for fluorescence measurements with our portable device, the smartphone camera recorded the emission light in a direction along the transmission direction (Fig. 3).

2.6. Multi-halide sensing

For proof of concept, we chose Cl^- and Br^- to demonstrate multi-halide sensing due to their abundance in natural aqueous environments and human body fluids. The Cl^- and Br^- were introduced by adding certain amounts of NaCl and LiBr to deionized (DI) water at various pH to prepare the artificial multi-halide solutions. In our previous work, we have tested various anions (OH^-, NO_3^-, ClO_4^-, CO_3^{2-}, SO_4^{2-}, PO_3^{2-}, PO_4^{3-}), cations (Li^+, Na^+, K^+, NH_4^+, Ca^{2+}, Mg^{2+}) and small molecules (acetate, citrate, glucose) on the fluorescence quenching of CA-Cys. All of them showed negligible influence on fluorescence quenching [43]. Therefore, the impact of the cations (Li^+ and Na^+) and SO_4^{2-} in the artificial multi-halide solutions on halide sensing is negligible. For multi-halide sensing with a fluorometer, standard curves for each halide were made by plotting I_0/I versus halide concentrations at two different pH (0.005 M H_2SO_4 (pH 2.3) and 0.1 M H_2SO_4 (pH 1.0)). As shown in Eqs. (2) and (3), the concentration of H^+ also affects I_0/I, resulting in a pH-dependent Stern-Volmer quenching constant i.e. $K_{sv(Q)}^* = K_{sv(Q)}/(K_{sv(H^+)}[H^+]+1)$. Therefore, when the pH difference of the two solutions is relatively large, $K_{sv(Q)1}^*$ and $K_{sv(Q)2}^*$ also significantly differ, improving the tolerance to noise and resulting in an improvement for sensitivity and accuracy. Standard fluorometer quartz cuvettes with a 1 cm light path were used for measurements. The volume of each solution was 2 mL constituting of 1 mL halide solution, 0.5 mL certain concentration of H_2SO_4 and 0.5 mL 0.4 OD CA-Cys solution (0.1 final OD, ~10 μM). Two artificial halide solutions were tested to solve the Cl^- and Br^- concentrations, and the results were compared with known concentrations. Each concentration had three replicates.

For fluorescence measurements with the smartphone-based portable device, the standard curves were made by using higher concentrations of halides due to the lowered measurement accuracy of the device. Quartz fluorometer microcuvettes with a 3 × 3 mm cross-section were used for the measurements. The volume of each solution was 200 μL, while the pH, ratio between components and concentration of CA-Cys were all the same as those in the fluorometer measurements. Two artificial halide solutions were tested to solve the Cl^- and Br^- concentrations and the results were compared with known concentrations. Each concentration had two replicates.

3. Results and discussion

3.1. Photophysical and optical properties of CA-Cys

The steady-state photoluminescent spectra showed that the maximum excitation wavelength of CA-Cys at a neutral state (pH > 2.4) was 348 nm and the corresponding maximum emission wavelength was 425 nm, while at an acidic state (pH < 2.4), the maximum excitation wavelength showed a bathochromic shift to 362 nm and the maximum emission wavelength also red-shifted to 443 nm with the intensity decreased due to the proton quenching effect (Fig. 2 (b)). Notably, neutral state (unquenched) CA-Cys showed a high quantum yield (90.52 ± 0.432%), which is attributed to its rigid molecular structure. The lifetime of neutral state CA-Cys was 10.06 ns [43], which is relatively long among pure organic fluorophores and might be a promising candidate for fluorescence lifetime imaging applications. Moreover, both neutral and acidic states of CA-Cys exhibited excellent photostability [43], ideal for delivery/handling in indoor or open areas under normal lighting conditions and suitable for applications requiring extended testing time, such as continuous environmental monitoring.

To better quantify the color changes between the neutral state and the acidic state of CA-Cys, the CIE 1931 chromaticity diagram and photos of two samples exemplifying the two states of CA-Cys were given in Fig. 2 (c). All human visual colors can be located in the CIE 1931 chromaticity diagram with their one-to-one corresponding coordinates. The CIE 1931 chromaticity coordinate of the neutral state CA-Cys was (0.154, 0.054), while that of the acidic state CA-Cys was (0.149, 0.089), which exhibited more cyan color due to the red shift of the entire emission spectrum.

3.2. Multi-halide sensing with a fluorometer

The standard curves of both Cl^- and Br^- at two different pH (0.005 M H_2SO_4 (pH 2.3) and 0.1 M H_2SO_4 (pH 1.0)) were obtained by plotting the $I_0/$
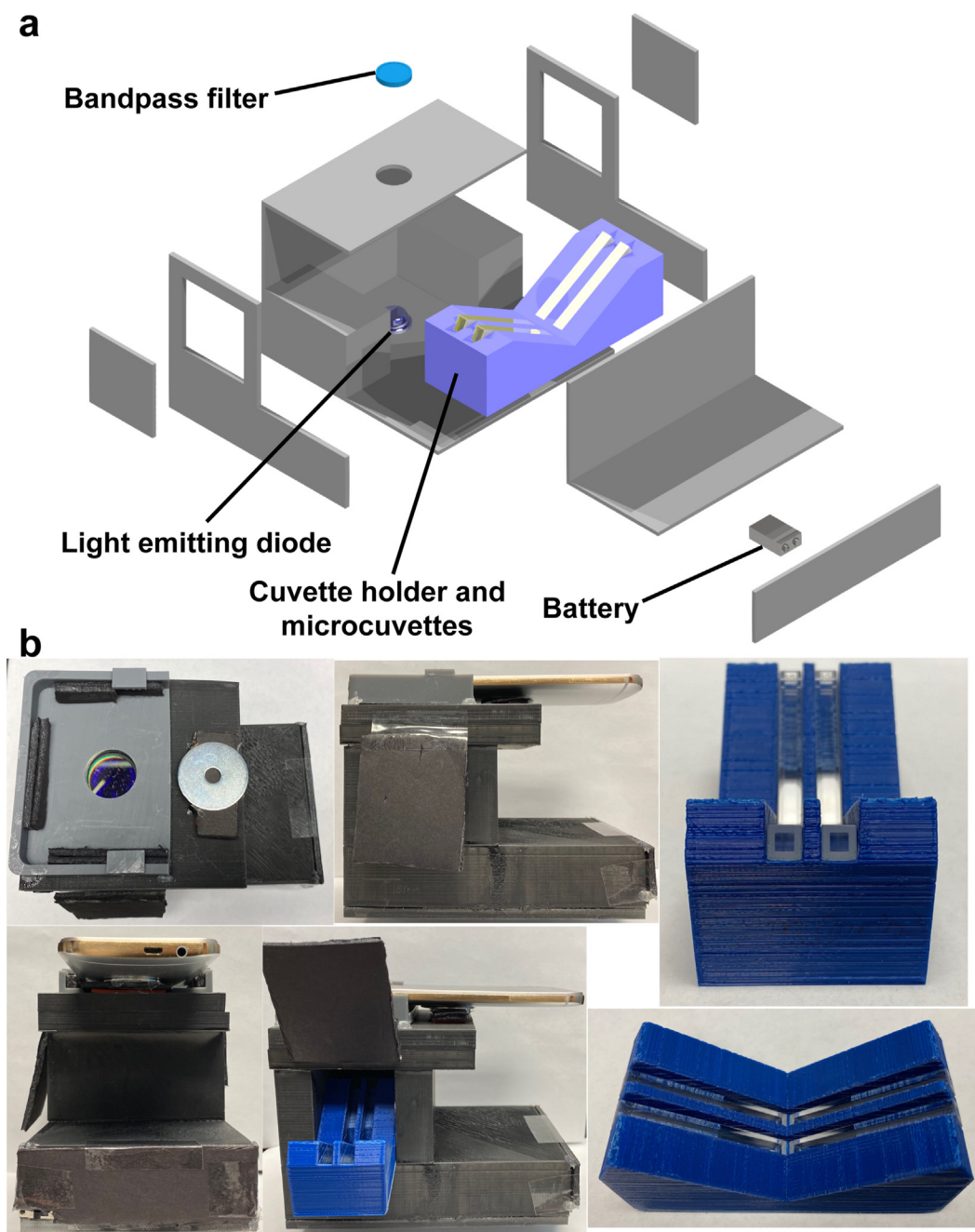
Fig. 3. Smartphone-based portable device. (a) Schematic diagram of the portable device. (b) Photos of the portable device (with/without smartphone), cuvette holder and microcuvettes.

I value versus halide concentration data points followed by a linear fit. When obtaining the standard curves of Cl^-, the Br^- concentration was kept constant at 0 and the Cl^- concentration was varied at a constant pH value and vice versa. Standard surfaces were also presented, which were defined by the Cl^- and Br^- standard curves at the same pH condition. The standard curves and standard surfaces of both Cl^- and Br^- at two pH are shown in Fig. 4 (a), (b) and (c). The slopes of Br^- were larger than those of Cl^- due to the stronger heavy atom effect. The R^2 values of the linear fit of the standard curves, which represent how well the linear regression is, were all greater than 0.99. The concentrations of Cl^- and Br^- in artificial solutions were calculated by solving the sets of equations. The ground truth, the experimentally retrieved values and the relative errors are shown in Table 1.

As shown in Table 1, the experimentally retrieved values matched well to the ground truth in all three artificial groups. As the Br^- concentration decreased, the relative errors increased. The results indicate

that our multi-halide sensing method with measurements using a commercial fluorometer is suitable for mM scale Cl^- and Br^- measurements and the results of sub-mM scale measurements might be unreliable under the current test conditions.

3.3. Multi-halide sensing with a portable device

The standard curves of both Cl^- and Br^- at two different pHs (0.005 M H_2SO_4 (pH 2.3) and 0.1 M H_2SO_4 (pH 1.0)) were also obtained using the portable device. The standard curves and standard surfaces of both Cl^- and Br^- at two pH are shown in Fig. 4 (d), (e) and (f). Similarly, the slopes of Br^- were larger than those of Cl^- due to the stronger heavy atom effect. The concentrations of Cl^- and Br^- in artificial solutions were calculated by solving the equation set. The ground truth, the experimentally retrieved values and the relative errors are summarized in Table 2.
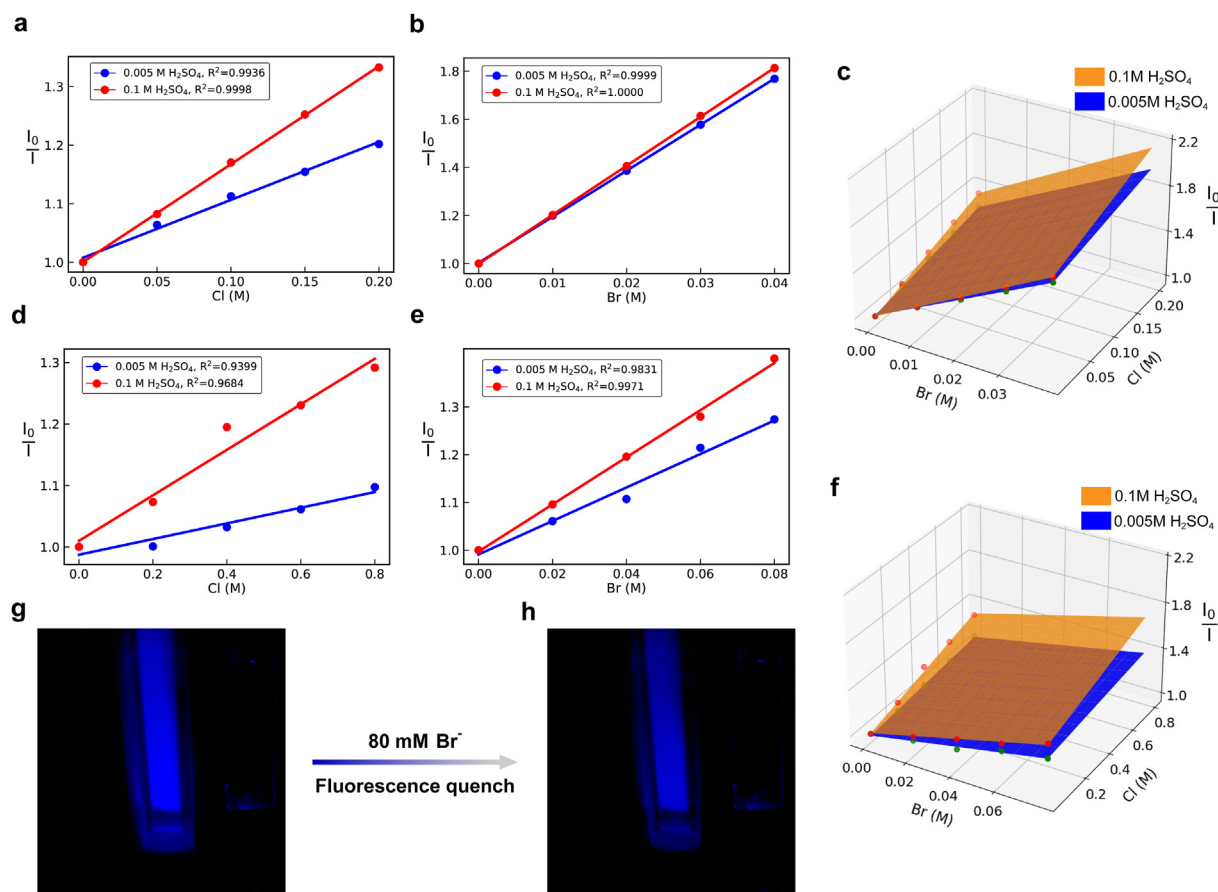
Fig. 4. Standard curves and surfaces of halide(s). (a) Standard curves of Cl^- at 0.005 M H_2SO_4 and 0.1 M H_2SO_4 (R^2 = 0.9936, 0.9998, respectively) measured using a fluorometer. (b) Standard curves of Br^- at 0.005 M H_2SO_4 and 0.1 M H_2SO_4 (R^2 = 0.9999, 1.000, respectively) measured using a fluorometer. (c) Standard surfaces of Cl^- and Br^- measured using a fluorometer. (d) Standard curves of Cl^- at 0.005 M H_2SO_4 and 0.1 M H_2SO_4 (R^2 = 0.9399, 0.9684, respectively) from portable device. (e) Standard curves of Br^- at 0.005 M H_2SO_4 and 0.1 M H_2SO_4 (R^2 = 0.9831, 0.9971, respectively) from portable device. (f) Standard surfaces of Cl^- and Br^- from portable device. (g) Image from portable device with 0 Cl^- and 0 Br^-. (h) Image from portable device with 0 Cl^- and 80 mM Br^-.

Table 1
Multi-halide test results from the fluorometer.

Artificial solution No.	Ground truth	Experimentally retrieved value	Relative error
1	100 mM Cl^-, 10 mM Br^-	96.51 mM Cl^-, 9.95 mM Br^-	Cl^- 3.49%, Br^- 0.5%
2	100 mM Cl^-, 5 mM Br^-	94.53 mM Cl^-, 5.54 mM Br^-	Cl^- 5.47%, Br^- 10.8%
3	100 mM Cl^-, 2.5 mM Br^-	95.83 mM Cl^-, 2.84 mM Br^-	Cl^- 4.17%, Br^- 13.6%

Table 2
Multi-halide test results from smartphone-based device.

Artificial solution No.	Ground truth	Experimentally retrieved value	Relative error
1	100 mM Cl^-, 20 mM Br^-	120.2 mM Cl^-, 16.32 mM Br^-	Cl^- 20.2%, Br^- 18.4%
2	200 mM Cl^-, 30 mM Br^-	202.67 mM Cl^-, 26.32 mM Br^-	Cl^- 1.34%, Br^- 12.27%

As shown in Table 2, the experimentally retrieved value matched well to the ground truth in more concentrated artificial group (200 mM Cl^-, 30 mM Br^-). As Cl^- and Br^- concentrations decreased, the relative error increased. Especially, the relative error of Cl^- increased significantly. The results obtained from the portable device are apparently worse than those from the fluorometer. The reason is that the measurement accuracy of the fluorometer is better than that of the portable device. This is often the difference between field and laboratory measurements. However, there is still room for improvements, such as introducing self-calibration of the light source and light path optimization.

3.4. Potential applications

The concentration of different halide ions varies significantly in the natural environment. In general, the concentrations followed the order of $[Cl^-] > [Br^-] > [I^-]$. For example, there are usually less Br^- than Cl^-, in

certain industrial wastewaters such as leaded gasoline (which has been eliminated worldwide since July 2021), pesticides, flame retardants, pharmaceuticals, photographic papers and certain chemical industrial wastewater [46–49]. The Br^- concentration can vary significantly from 11.3 to 3070 mg/L (0.14–38.42 mM) [46,48,50,51]. As mentioned in the introduction, the brominated products from Br^- can cause severe health issues which need to be closely monitored. Additionally, Cl^- and Br^- are two of the main interference ions in chemical oxygen demand (COD) measurement, which is a well-recognized parameter in wastewater treatment and water quality management [46,51]. Especially, Cl^- concentration is one of the typical wastewater parameters and has been reported to have a positive correlation with residual adsorbable organic halides concentrations in industrial wastewater [52]. Therefore, it is important to know the concentration of both Cl^- and Br^-. However, the current standard procedure of measuring Cl^-, which is based on titration and colorimetric measurements (thiocyanate method, ISO 15923–1:2013), is significantly interfered by Br^- above 30 mg/L and suffers from complicated and laborious sample preparation. Therefore,

industrial wastewater measurement is a niche application for our system that is capable of convenient and simultaneous multi-halide detections.

In addition to multi-halide sensing, our system has a proven high sensitivity and selectivity for single halide ion sensing. The results presented in this work and our previous work showed that the detection limit for Cl^- (sub-mM) or Br^- (tens of μM) only is within the physiological or pathological concentration ranges in human body fluids, such as sweat. For example, the normal Cl^- and Br^- concentrations of human sweat are below 30 mM and 10 μM, respectively, while for cystic fibrosis patients, the sweat Cl^- and Br^- concentration can be higher than 60 mM and 70 μM [21]. The normal urine Cl^- concentration is below 15 mM [53] while the normal serum Cl^- concentration is ranging from 96 to 106 mM [54]. Therefore, our CA-Cys-based sensing system is promising for the diagnosis of diseases that are characteristic of abnormal halide concentrations, such as cystic fibrosis, metabolic alkalosis, Addison's disease, and amyotrophic lateral sclerosis (ALS) [4–6,55].

There is still a need to continue improving the detection limit of the citrate-based multi-halide sensors, particularly for Br^- and I^-. For example, the concentration of Cl^- in seawater is around 546 mM [56], while the concentration of Br^- is around 844 μM [56]. The seawater I^- concentration ranges from 236 nM (near the shore and in the ocean surface and bottom waters) to 7.9 nM (deep ocean water) [57]. The halide concentrations are much lower in non-brine natural waters and human body fluids. Thus, the improved detection limit can expand the multi-halide sensing application scenarios from wastewater to seawater and even groundwater and human body fluids. For example, the current gold standard for cystic fibrosis diagnosis is the sweat Cl^- test. However, the sweat Cl^- concentration between 30 and 59 mM is the gray zone of diagnosis of cystic fibrosis. Several works showed that the sweat or serum Br^- concentrations in CF gene carriers and patients are higher than those in normal people [21,22]. The Br^- concentration may work as an extra diagnostic parameter and help determine whether some gray-zone patients are CF positive. Thus, an improved detection limit could bring a fast and low-cost measurement of both sweat Cl^- and Br^- simultaneously to narrow the diagnosis gray zone. There are several potential ways to improve the detection limit. From a material point of view, dimerization of halide sensitive moiety might increase the Stern-Volmer quenching constant (K_{sv}), resulting in an improvement of the halide detection limit. Meanwhile, the extension of the conjugation system will enhance photon absorption, which is commonly represented by the molar extinction coefficient (ε, $cm^{-1}M^{-1}$) and boost fluorescence brightness. For example, comparing lucigenin that contains two halide sensitive moieties in one molecule to other commercial halide indicators that only have one halide sensitive moiety, such as SPQ, MQAE and MEQ, lucigenin possesses 7400 $cm^{-1}M^{-1}$ of ε and 390 M^{-1} of K_{sv} while SPQ has 3700 $cm^{-1}M^{-1}$ of ε and 118 M^{-1} of K_{sv}, MQAE has 2800 $cm^{-1}M^{-1}$ of ε and 200 M^{-1} of K_{sv} and MEQ has 3900 $cm^{-1}M^{-1}$ of ε and 145 M^{-1} of K_{sv} [58–60]. Thus, the dimerization of CA-Cys may yield a high K_{sv} and improve the detection limit. There is also a room to improve the detection limit from a device design aspect. As mentioned before, the fluorescence signal is collected in a direction perpendicular to the incident light beam in the fluorometer, mitigating the influence of strong excitation light. Therefore, results from the device will show better sensitivity and linearity if the smartphone camera is also placed perpendicular to the direction of the incident light. Furthermore, lenses could also be mounted between LED and cuvettes to better focus the excitation light on the sample. In this way, a stronger fluorescence can be recorded, and the signal-to-noise ratio may be improved. Moreover, some self–calibration processes may be utilized on camera, resulting in more matched photos and therefore, more precise detection.

4. Conclusions

In summary, we have developed a new fluorometric multi-halide sensing method and a smart phone-based portable device using a single citrate-based fluorophore. With the unique feature of variable halide

sensitivity of our novel fluorophore at different pH, multiple equations can be used to solve each halide concentration. Artificial halides solutions have been tested with both a commercial fluorometer and a portable device. The results have proven the feasibility of our method. Although the current detection limits of multi-halides were relatively high (mM scale), it already proves its potential for industrial applications such as halide wastewater monitoring. The ability to achieve simultaneous multi-halide concentration determination with a single fluorophore could pave a new way for future potential applications such as point-of-care, low-cost sweat analysis and seawater and groundwater monitoring. We believe that by optimizing or designing new fluorescent probes with similar multi-halide sensitive core structures and having increased halide sensitivity and better detection limit, there is a great potential to apply the multi-halide sensing method to various applications mentioned above.

CRediT authorship contribution statement

Dingbowen Wang: Formal analysis. **Tunan Xia:** Formal analysis. **Yuqi Wang:** Formal analysis. **Yizhu Chen:** Formal analysis. **Chenji Zhang:** Formal analysis. **William Murray:** Formal analysis. **Zhiwen Liu:** Formal analysis. **Jian Yang:** Formal analysis.

Declaration of competing interest

The authors declare the following financial interests/personal relationships which may be considered as potential competing interests:

Dr. Yang and the Pennsylvania State University have a financial interest in Acuitive Technologies, Inc. and Aleo BME, Inc. These interests have been reviewed by the University's Institutional and Individual Conflict of Interest Committees and are currently being managed by the University.

Acknowledgements

References

[1] W. D'Alessandro, S. Bellomo, F. Parello, L. Brusca, M. Longo, Survey on fluoride, bromide and chloride contents in public drinking water supplies in Sicily (Italy), Environ. Monit. Assess. 145 (2008) 303–313.

[2] M. Flury, A. Papritz, Bromide in the natural environment: occurrence and toxicity, J. Environ. Qual. 22 (1993) 747–758.

[3] W.E. Federation, A. Association, Standard Methods for the Examination of Water and Wastewater, American Public Health Association (APHA), Washington, DC, USA, 2005.

[4] S.A. Blythe, P.M. Farrell, Advances in the diagnosis and management of cystic fibrosis, Clin. Biochem. 17 (1984) 277–283.

[5] S. Watanabe, T. Kimura, K. Suenaga, S. Wada, K. Tsuda, S. Kasama, T. Takaoka, K. Kajiyama, M. Takeda, H. Yoshikawa, Decreased chloride levels of cerebrospinal fluid in patients with amyotrophic lateral sclerosis, J. Neurol. Sci. 285 (2009) 146–148.

[6] D. Pahari, W. Kazmi, G. Raman, S. Biswas, Diagnosis and management of metabolic alkalosis, J. Indian Med. Assoc. 104 (2006) 630–634, 636.

[7] P.N. Taylor, D. Albrecht, A. Scholz, G. Gutierrez-Buey, J.H. Lazarus, C.M. Dayan, O.E. Okosieme, Global epidemiology of hyperthyroidism and hypothyroidism, Nat. Rev. Endocrinol. 14 (2018) 301–316.

[8] A.S. McCall, Christopher F. Cummings, G. Bhave, R. Vanacore, A. Page-McCaw, Billy G. Hudson, Bromine is an essential trace element for assembly of collagen IV scaffolds in tissue development and architecture, Cell 157 (2014) 1380–1392.

[9] Bromide in Drinking-Water: Background Document for Development of WHO Guidelines for Drinking-Water Quality, World Health Organization, 2009.

[10] T.V. Luong, C.J. Peters, R. Perry, Influence of bromide and ammonia upon the formation of trihalomethanes under water-treatment conditions, Environ. Sci. Technol. 16 (1982) 473–479.

[11] G. Amy, C. Douville, B. Daw, J. Sohn, C. Galey, D. Gatel, J. Cavard, Bromate formation under ozonation conditions to inactivate Cryptosporidium, Water Sci. Technol. 41 (2000) 61–66.

[12] A.E. Munson, L.E. Sain, V.M. Sanders, B.M. Kauffmann, K.L. White Jr., D.G. Page, D.W. Barnes, J.F. Borzelleca, Toxicology of organic drinking water contaminants:

trichloromethane, bromodichloromethane, dibromochloromethane and tribromomethane, Environ. Health Perspect. 46 (1982) 117–126.

[13] M.H. George, G.R. Olson, D. Doerfler, T. Moore, S. Kilburn, A.B. De Angelo, Carcinogenicity of bromodichloromethane administered in drinking water to male F344/N rats and B6C3F1 mice, Int. J. Toxicol. 21 (2002) 219–230.

[14] R.L. Balster, J.F. Borzelleca, Behavioral toxicity of trihalomethane contaminants of drinking water in mice, Environ. Health Perspect. 46 (1982) 127–136.

[15] J. Andrews, H. Nichols, J. Schmid, L. Mole, E. Hunter III, G. Klinefelter, Developmental toxicity of mixtures: the water disinfection by-products dichloro-, dibromo-and bromochloro acetic acid in rat embryo culture, Reprod. Toxicol. 19 (2004) 111–116.

[16] N. Weber, T. Higuchi, J. Tessari, D.R. Veeramachaneni, Evaluation of the effects of water disinfection by-products, bromochloroacetic and dibromoacetic acids, on frog embryogenesis, J. Toxicol. Environ. Health 67 (2004) 929–939.

[17] Y. Kurokawa, S. Takayama, Y. Konishi, Y. Hiasa, S. Asahina, M. Takahashi, A. Maekawa, Y. Hayashi, Long-term in vivo carcinogenicity tests of potassium bromate, sodium hypochlorite, and sodium chlorite conducted in Japan, Environ. Health Perspect. 69 (1986) 221–235.

[18] S.D. Richardson, A.D. Thruston, C. Rav-Acha, L. Groisman, I. Popilevsky, O. Juraev, V. Glezer, A.B. McKague, M.J. Plewa, E.D. Wagner, Tribromopyrrole, brominated acids, and other disinfection byproducts produced by disinfection of drinking water rich in bromide, Environ. Sci. Technol. 37 (2003) 3782–3793.

[19] S.N. Davis, D.O. Whittemore, J. Fabryka-Martin, Uses of chloride/bromide ratios in studies of potable water, Groundwater 36 (1998) 338–350.

[20] Z. Szczepański, Sweat bromide test—a diagnostic tool for mucoviscidosis, Z. Kinderheilkd. 113 (1972) 297–302.

[21] M.E. Miller, J.M. Cosgriff, R.H. Schwartz, Sweat Bromide Excretion in Cystic Fibrosis Patients, Obligate Carriers, and Controls, 1985.

[22] H. Theile, H. Gressmann, P. Winiecki, Detection of cystic fibrosis heterozygotes using a modified loading with bromide, Hum. Genet. 69 (1985) 277–280.

[23] J. Brodkey, G. Gibbs, Sweat iodide excretion in patients with cystic fibrosis of the pancreas, J. Appl. Physiol. 15 (1960) 501–502.

[24] H.A. Olszowy, J. Rossiter, J. Hegarty, P. Geoghegan, M. Haswell-Elkins, Background levels of bromide in human blood, J. Anal. Toxicol. 22 (1998) 225–230.

[25] K.D. McClatchey, Clinical Laboratory Medicine, Lippincott Wiliams & Wilkins, 2002.

[26] C.A. Burtis, E.R. Ashwood, D.E. Bruns, Tietz Textbook of Clinical Chemistry and Molecular Diagnostics-E-Book, Elsevier Health Sciences, 2012.

[27] D. Wegmann, H. Weiss, D. Ammann, W. Morf, E. Pretsch, K. Sugahara, W. Simon, Anion-selective liquid membrane electrodes based on lipophilic quaternary ammonium compounds, Microchim. Acta 84 (1984) 1–16.

[28] P. Bray, G. Clark, G. Moody, J. Thomas, Sweat testing for cystic fibrosis: errors associated with the in-situ sweat test using chloride ion selective electrodes, Clin. Chim. Acta 80 (1977) 333–338.

[29] R.S. Blume, J.D. MacLowry, S.M. Wolff, Limitations of chloride determination in the diagnosis of bromism, N. Engl. J. Med. 279 (1968) 593–595.

[30] D.L. Wise, Bioinstrumentation and Biosensors, CRC Press, 1991.

[31] A. Lynch, D. Diamond, M. Leader, Point-of-need diagnosis of cystic fibrosis using a potentiometric ion-selective electrode array, Analyst 125 (2000) 2264–2267.

[32] R.D. Rocklin, E.L. Johnson, Determination of cyanide, sulfide, iodide, and bromide by ion chromatography with electrochemical detection, Anal. Chem. 55 (1983) 4–7.

[33] A. Verkman, Development and biological applications of chloride-sensitive fluorescent indicators, Am. J. Physiol. Cell Physiol. 259 (1990) C375–C388.

[34] T. Riis-Johannessen, K. Schenk, K. Severin, Turn-off-and-on: chemosensing ensembles for sensing chloride in water by fluorescence spectroscopy, Inorg. Chem. 49 (2010) 9546–9553.

[35] M. Porel, V. Ramalingam, M.E. Domaradzki, V.G. Young, V. Ramamurthy, R.S. Muthyala, Chloride sensing via suppression of excited state intramolecular proton transfer in squaramides, Chem. Commun. 49 (2013) 1633–1635.

[36] M.M. Watt, J.M. Engle, K.C. Fairley, T.E. Robitshek, M.M. Haley, D.W. Johnson, Off-on" aggregation-based fluorescent sensor for the detection of chloride in water, Org. Biomol. Chem. 13 (2015) 4266–4270.

[37] J.R. Lakowicz, Principles of Fluorescence Spectroscopy, Springer science & business media, 2013.

[38] C.D. Geddes, K. Apperson, J. Karolin, D.J. Birch, Chloride-sensitive fluorescent indicators, Anal. Biochem. 293 (2001) 60–66.

[39] O. Markova, M. Mukhtarov, E. Real, Y. Jacob, P. Bregestovski, Genetically encoded chloride indicator with improved sensitivity, J. Neurosci. Methods 170 (2008) 67–76.

[40] T. Kuner, G.J. Augustine, A genetically encoded ratiometric indicator for chloride: capturing chloride transients in cultured hippocampal neurons, Neuron 27 (2000) 447–459.

[41] R.M. Wachter, S.J. Remington, S. Jayaraman, P. Haggie, A. Verkman, Mechanism and cellular applications of a green fluorescent protein-based halide sensor, J. Biol. Chem. 275 (2000) 6047–6050.

[42] R.M. Wachter, S.J. Remington, Sensitivity of the yellow variant of green fluorescent protein to halides and nitrate, Curr. Biol. 9 (1999) R628–R629.

[43] J.P. Kim, Z. Xie, M. Creer, Z. Liu, J. Yang, Citrate-based fluorescent materials for low-cost chloride sensing in the diagnosis of cystic fibrosis, Chem. Sci. 8 (2017) 550–558.

[44] Z. Xie, J.P. Kim, Q. Cai, Y. Zhang, J. Guo, R.S. Dhami, L. Li, B. Kong, Y. Su, K.A. Schug, J. Yang, Synthesis and characterization of citrate-based fluorescent small molecules and biodegradable polymers, Acta Biomater. 50 (2017) 361–369.

[45] G.F. Pauli, S.-N. Chen, C. Simmler, D.C. Lankin, T. Gödecke, B.U. Jaki, J.B. Friesen, J.B. McAlpine, J.G. Napolitano, Importance of purity evaluation and the potential of quantitative 1H NMR as a purity assay, J. Med. Chem. 57 (2014) 9220–9231.

[46] X. Shi, S. Huang, T.S. Yeap, S.L. Ong, H.Y. Ng, A method to eliminate bromide interference on standard COD test for bromide-rich industrial wastewater, Chemosphere 240 (2020) 124804.

[47] M.B. Heeb, J. Criquet, S.G. Zimmermann-Steffens, U. Von Gunten, Oxidative treatment of bromide-containing waters: formation of bromine and its reactions with inorganic and organic compounds—a critical review, Water Res. 48 (2014) 15–42.

[48] Z. Li, Y. Sheng, Q. Sun, Y. Qu, Effect of bromide ion in water on chemical oxygen demand determination, Chin. J. Environ. Eng. 9 (2015) 5125–5132.

[49] F. Soltermann, C. Abegglen, C. Gotz, U. Von Gunten, Bromide sources and loads in Swiss surface waters and their relevance for bromate formation during wastewater ozonation, Environ. Sci. Technol. 50 (2016) 9825–9834.

[50] G.-m. Cao, M. Sheng, C. Zhong, F.-z. Zhou, Effect of bromide ion in industrial wastewater on chemical oxygen demand determination, China Water & Wastewater 23 (2007) 85.

[51] I. Cardona, H.I. Park, L.S. Lin, Improved COD measurements for organic content in flowback water with high chloride concentrations, Water Environ. Res. 88 (2016) 210–216.

[52] H. Milh, K. Van Eyck, B. Bastiaens, S. De Laet, D. Leysen, D. Cabooter, R. Dewil, Predicting residual adsorbable organic halides concentrations in industrial wastewater using typical wastewater parameters, Water 12 (2020) 1653.

[53] K.S. Kamel, J.H. Ethier, R.M.A. Richardson, R.A. Bear, M.L. Halperin, Urine electrolytes and osmolality: when and how to use them, Am. J. Nephrol. 10 (1990) 89–102.

[54] G. Morrison, Serum Chloride, Clinical Methods: the History, Physical, and Laboratory Examinations, third ed., 1990.

[55] Z. Szczepański, Sweat bromide test — a diagnostic tool for mucoviscidosis, Z. Kinderheilkd. 113 (1972) 297–302.

[56] A.G. Dickson, C. Goyet, Handbook of Methods for the Analysis of the Various Parameters of the Carbon Dioxide System in Sea Water, Oak Ridge National Lab., TN (United States), 1994. Version 2.

[57] K. Ito, Determination of iodide in seawater by ion chromatography, Anal. Chem. 69 (1997) 3628–3632.

[58] J. Biwersi, B. Tulk, A.S. Verkman, Long-wavelength chloride-sensitive fluorescent indicators, Anal. Biochem. 219 (1994) 139–143.

[59] J. Biwersi, A.S. Verkman, Cell-permeable fluorescent indicator for cytosolic chloride, Biochemistry 30 (1991) 7879–7883.

[60] A. Verkman, M. Sellers, A. Chao, T. Leung, R. Ketcham, Synthesis and characterization of improved chloride-sensitive fluorescent indicators for biological applications, Anal. Biochem. 178 (1989) 355–361.